

Lifetime and predissociation yield of $^{14}\text{N}_2$ $b^1\Pi_u(v=1)$

J. P. Sprengers and W. Ubachs

Department of Physics and Astronomy, Laser Centre, Vrije Universiteit, De Boelelaan 1081, 1081 HV Amsterdam, The Netherlands

A. Johansson, A. L'Huillier, and C.-G. Wahlström

Department of Physics, Lund Institute of Technology, P.O. Box 118, S-221 00 Lund, Sweden

R. Lang^{a)}

Department of Physics and Astronomy, Laser Centre, Vrije Universiteit, De Boelelaan 1081, 1081 HV Amsterdam, The Netherlands and FOM-Institute for Atomic and Molecular Physics, Kruislaan 407, 1098 SJ Amsterdam, The Netherlands

B. R. Lewis and S. T. Gibson

Research School of Physical Sciences and Engineering, The Australian National University, Canberra, ACT, 0200, Australia

(Received 29 September 2003; accepted 23 February 2004)

The lifetime of the $b^1\Pi_u(v=1)$ state in $^{14}\text{N}_2$ has been determined experimentally using a laser-based pump-probe scheme and an exceptionally long lifetime of 2.61 ns was found. Semiempirical close-coupling calculations of the radiative lifetime, which include Rydberg-valence interactions in the singlet manifold, are consistent with this large value, giving a value of 3.61 ns and suggesting a predissociation yield of $\sim 28\%$ for this level of the b state. © 2004 American Institute of Physics. [DOI: 10.1063/1.1704640]

I. INTRODUCTION

The dipole-allowed absorption spectrum of molecular nitrogen sets in at wavelengths $\lambda < 100$ nm and is governed by transitions from the ground state $X^1\Sigma_g^+$ to two valence states, $b^1\Sigma_u^+$ and $b^1\Pi_u$, two np -Rydberg series $c'_{n+1}^1\Sigma_u^+$ and $c_n^1\Pi_u$, converging on the ionic ground state, and an ns -Rydberg series $o_n^1\Pi_u$, converging on the first-excited ionic state. The combined effect of these mutually interacting states is to shield the Earth's atmosphere below 100 km from hazardous extreme ultraviolet (XUV) radiation. Knowledge of the competition between the N_2 de-excitation processes of fluorescence and predissociation, obtained from electron-impact¹⁻³ or photoexcitation experiments (see below) is of great practical importance in view of the roles of these processes in atmospheric radiative transport⁴ and ionospheric chemistry.

Furthermore, studies of the spectroscopy and decay dynamics of N_2 states in the XUV are important in providing advances in our understanding of fundamental molecular problems. In particular, the $^1\Pi_u$ symmetry states of N_2 present a textbook example of Rydberg-valence and Rydberg-Rydberg interactions, widely discussed previously for the main isotopomer $^{14}\text{N}_2$ in Refs. 5-9. The dipole-allowed spectrum of $^{14}\text{N}_2$ has been extensively studied, but there are sufficient outstanding problems, e.g., the determination of absolute oscillator strengths, for such studies to be ongoing.¹⁰ Dipole-allowed ionization spectra for the isotopomers $^{15}\text{N}_2$ and, to a lesser extent, $^{14}\text{N}^{15}\text{N}$ have also been studied recently by Sprengers *et al.*¹¹

An understanding of the predissociation mechanisms for the $^1\Pi_u$ (and $^1\Sigma_u^+$) states remains one of the major outstanding problems in N_2 structure and dynamics. While it is likely that the ultimate dissociation channel is a $^3\Pi_u$ continuum, despite attempts over many years to establish these mechanisms, no quantitative predissociation model exists to explain the seemingly erratic dependence of $^1\Pi_u$ predissociation rates on the vibrational quantum number, in particular, for the $b^1\Pi_u$ valence state. The development of such a model requires, not only an improved theoretical understanding of the interactions between the $^1\Pi_u$ states of N_2 (Rydberg-valence, Rydberg-Rydberg, and valence-valence), but also a reliable experimental database for all isotopomers. Considering the wide range of applicable predissociation rates, such a database would benefit from direct (Doppler-free) linewidth measurements, for the broader levels, and direct lifetime measurements, for the narrower levels. This latter need is addressed in this work for the narrow $b^1\Pi_u(v=1)$ state in $^{14}\text{N}_2$.

Several experimental studies have been performed on linewidths and lifetimes of the $^1\Pi_u$ states, but the picture is presently incomplete and there are many inconsistencies in the results. Linewidths for the lower-energy $^1\Pi_u$ states, including the low- v levels of the b state, were determined by Leoni and Dressler¹² who analyzed photoelectric scans of the absorption bands taken at many pressures. Predissociation lifetimes for excited states of $^1\Pi_u$ symmetry were determined by Ubachs and co-workers¹³⁻¹⁶ using narrowband XUV-laser excitation, while Kawamoto *et al.*¹⁷ studied predissociation of the $c_3(v=1)$ level using near-infrared excitation from the long-lived $a''^1\Sigma_g^+$ metastable state. Helm, Cosby, and co-workers determined dissociation quantum

^{a)}Present address: Max Planck Institute for Chemistry, Department of Airchemistry/NWG, Postfach 3060, 55020 Mainz, Germany.

yields of somewhat higher-lying vibronic states of ${}^1\Pi_u$ symmetry using laser-induced photofragment spectroscopy, after population of the metastable state via charge exchange.^{18–22} Buijsse and van der Zande also used the photofragment technique,²³ as well as the Hanle effect,²⁴ to investigate in detail rotational-state effects in the predissociation of the $e\,{}^1\Pi_u(v=0)$ state, which is also known as $c_4\,{}^1\Pi_u(v=0)$. Direct time-domain lifetime measurements of N_2 excited states have also been performed using short pulses from a synchrotron source; lifetimes of $o_3(v=2)$ and $b(v=0-1)$ were determined.²⁵

From an atmospheric perspective, there are two vibronic states that behave differently from all the others. Both the $c_4'\,{}^1\Sigma_u^+(v=0)$ and $b\,{}^1\Pi_u(v=1)$ states predissociate only to a minor extent, and XUV radiation is redistributed and scattered after excitation of these states. While the $c_4'\,{}^1\Sigma_u^+(v=0)$ Rydberg state radiates 90% back to the $X\,{}^1\Sigma_g^+(v=0)$ ground state, absorption into the $b\,{}^1\Pi_u(v=1)$ valence state induces fluorescence that is shifted to longer wavelengths. Accurate measurements of these lifetimes may help to elucidate the competition between predissociation and radiation in N_2 in the Earth's atmosphere.

In the present study, a picosecond laser system is used in a pump-probe configuration to study the lifetime of the $b\,{}^1\Pi_u(v=1)$ level in ${}^{14}N_2$. This study follows previous work²⁶ on lifetime measurements for the $c_4'\,{}^1\Sigma_u^+(v=0-2)$ states of ${}^{14}N_2$ and is part of a collaborative experimental and theoretical program intended to unravel the Rydberg-valence and singlet-triplet interactions of N_2 in the 100 000–110 000 cm^{-1} region. A theoretical model, based on Rydberg-valence interaction, is used to provide an explanation for the exceptionally long $b(v=1)$ lifetime found experimentally.

II. EXPERIMENTAL METHOD AND DATA ANALYSIS

A detailed description of the picosecond XUV-radiation source, the pump-probe 1XUV+1UV two-photon ionization scheme for direct time-domain measurements of excited-state lifetimes, and its application to excited states in N_2 , has been given previously.²⁶ Briefly, the infrared (IR) output of a distributed-feedback dye laser (DFDL), pumped by the frequency doubled output of a mode-locked Nd:YAG laser, was amplified in a titanium-sapphire crystal and frequency doubled to the ultraviolet (UV) in a KD*P crystal. Higher harmonic generation was then achieved by focusing the UV beam and the remaining IR beam into a pulsed krypton jet. To reach the desired wavelength, the eighth harmonic of the IR beam was produced by wave-mixing IR and UV photons; one of the processes yielding the eighth harmonic is $\nu_{XUV} = 3\nu_{UV} + 2\nu_{IR}$. The eighth harmonic was selected by a spherical grating, sent to the interaction region, refocused and crossed with a pulsed N_2 beam. The output of the DFDL was tuned by varying the temperature of the dye solution, allowing the XUV to be scanned over an absorption in N_2 . The XUV pump photon excited the molecules from the ground state to the excited state under investigation, while a delayable probe beam, the frequency tripled 355-nm output of the same mode-locked Nd:YAG laser, was focused into the interaction region, ionizing the excited N_2 molecules.

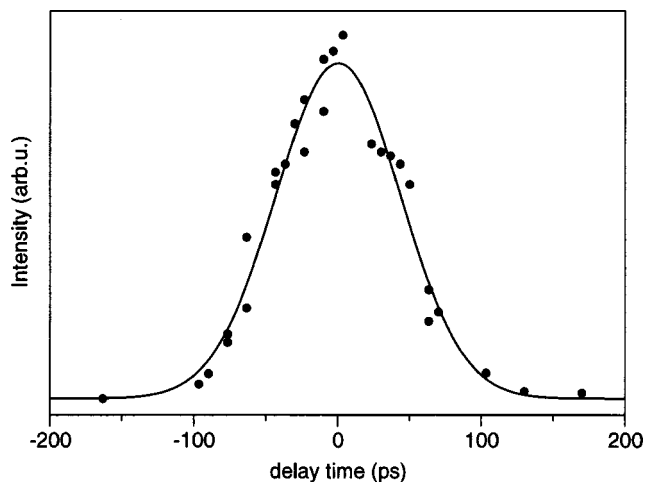


FIG. 1. Pump-probe delay scan with the XUV laser fixed at $\lambda = 96.56$ nm, probing the short-lived $b\,{}^1\Pi_u(v=4)$ level in ${}^{14}N_2$. The data have been centered around $\Delta T=0$ and fitted to a Gaussian, yielding an effective instrument width of 107 ps FWHM.

The resulting ions were accelerated by an electric field, passed through a time-of-flight (TOF) analyzer, and detected by an electron multiplier. Lifetime measurements were performed by temporally delaying the UV pulse with an optical rail and by measuring the intensity of the corresponding ion signal, which was averaged over 300 pulses. 1XUV+1UV ionization spectra of the excited states studied were obtained by scanning the XUV wavelength with zero time delay between the XUV and UV pulses.

Since an unexpectedly long lifetime was found for the $b\,{}^1\Pi_u(v=1)$ state in ${}^{14}N_2$, two dedicated measurement series were performed on the $b\,{}^1\Pi_u(v=1)$ state in ${}^{14}N_2$ with a two year time interval to verify the results. Measurements on the possible effects of radiation trapping were also performed for the $c_4'\,{}^1\Sigma_u^+(v=0)$ state, which has a larger oscillator strength, and which decays 90% into the $v=0$ level of the ground state. For this state, radiative trapping should be a much stronger effect, but no sign of increased lifetime was observed in the pressure range used. Since radiative decay of the $b(v=1)$ state is distributed over a vibrational manifold, with only $\sim 10\%$ decay to the $v=0$ ground-state level, the effects of radiative trapping should be smaller than for $c_4'(v=0)$.

An important limiting characteristic of the laser system is its bandwidth of $\Delta\lambda_{XUV} \approx 0.01$ nm in the XUV domain, which does not allow for full resolution of rotational structure in the N_2 bands. Nevertheless, the laser can be set to probe a limited number of lines within the band envelope, thus allowing for some rotational sensitivity. Previously, the temporal resolution of the apparatus was estimated from streak camera measurements of the IR laser pulses used for the generation of the XUV radiation via harmonic upconversion.²⁶ Here, in Fig. 1, we show a pump-probe delay scan for the $b(v=4)$ state of N_2 which is known to have a lifetime of 11–18 ps.^{13,16} The resulting convoluted width of 107 ps full-width at half-maximum (FWHM) represents, in fact, the instrument function of our pump-probe setup in the temporal domain. This value is in good agreement with an

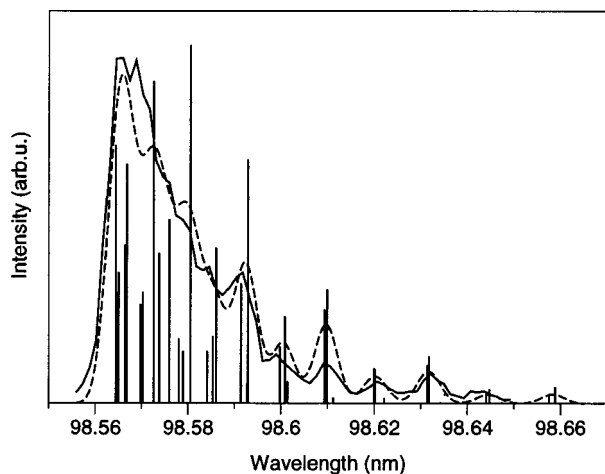


FIG. 2. Spectrum of the $b^1\Pi_u-X^1\Sigma_g^+(1,0)$ band in $^{14}\text{N}_2$. Full line: observed spectrum. Dashed line: calculated spectrum at $T=80$ K. Vertical sticks: line strengths of individual rotational lines.

actual measurement of pulse durations by a streak camera yielding a convoluted width of 95 ps.²⁶

Several fitting procedures were applied to the lifetime decay curves to derive estimates for the decay times and their uncertainties. The first method was analogous to that of Ref. 26, involving Monte Carlo simulations of the distribution of errors. Furthermore, the rate-equation model used in Ref. 27 and a method similar to that in Ref. 28 were applied.

Simulations of the recorded excitation spectra were made by convolving a stick spectrum, representing the relative rotational line strengths, with the bandwidth of the laser system. A rotational temperature of 80 K, together with appropriate Hönl–London factors, was employed and account was taken of the effect of nuclear-spin statistics on the rotational line strengths. The ranges of J levels probed during the lifetime measurements were estimated from the calculated spectra. The simulated spectrum of $b(v=1)$, in comparison with the experimental spectrum, is shown in Fig. 2. Some rotational structure is resolved experimentally for higher J levels, mainly because the R , Q , and P lines accidentally coincide. We note that our simulations are somewhat crude, not including the effects of Rydberg–valence, and $^1\Pi_u-^1\Sigma_u^+$ interactions on the rotational line strengths, nor the effects of J -dependent predissociation on the ionization quantum yield. These effects are likely to be small, however, for $b(v=1)$, the main subject of this study.

III. RESULTS AND DISCUSSION

A typical $b(v=1)$ decay transient is reproduced in Fig. 3. No evidence for a rotational dependence of the lifetime was found. Most measurements were performed near 98.57 nm, thus probing low J levels (see Fig. 2). A mean lifetime of 2635 ± 150 ps was found in the first measurement campaign, which yielded nine independent decay transients in the range 2359–2841 ps, consistent with a statistical distribution. During the second independent validation campaign, lifetimes of 2525 ± 150 ps were observed, an average over three measurements, confirming the long lifetime. A statistical analysis of all measurements yielded a final value of 2610 ± 100 ps.

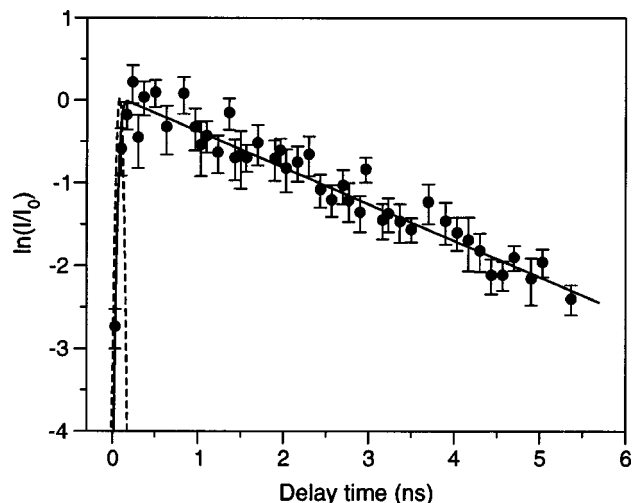


FIG. 3. Lifetime decay measurement for the $b^1\Pi_u(v=1)$ state of $^{14}\text{N}_2$. Full line: fit to observed data. Dashed line: time response function of the two laser pulses combined.

In previous studies, values for the lifetime of $b(v=1)$ in $^{14}\text{N}_2$ were determined as 1700 ± 250 ps (Ref. 25) and 1100 ± 300 ps.¹⁶ In the latter study, the linewidths of single rotational levels were investigated. In Ref. 16, it was stated that the wavelength resolution of the XUV laser was barely sufficient to enable the deconvolution of molecular lifetime effects from the observed widths. Furthermore, the possibility of hyperfine structure should be considered. Here, we conclude that the estimate of the instrument width in Ref. 16 was too optimistic. The picosecond XUV laser at Lund certainly provides much better accuracy for lifetimes in the dynamic range >500 ps, and hence the present value should be more trustworthy. For the discrepancy with the value obtained by Oertel *et al.*,²⁵ we have no explanation.

It is of interest, especially in view of this discrepancy, to see whether the long $b(v=1)$ lifetime determined here is compatible with estimates of the radiative lifetime of this level based on known oscillator strengths.

The relationship between the band oscillator strength $f_{v'v''}$ and the corresponding radiative decay channel is given by²⁹

$$f_{v'v''} = \frac{2 - \delta_{0\Lambda'}}{2 - \delta_{0\Lambda''}} 4\pi\epsilon_0 \frac{m_e c}{8\pi^2 e^2} \lambda_{v'v''}^2 A_{v'v''}, \quad (1)$$

where v' and v'' denote vibrational levels in the upper and lower electronic states, $\lambda_{v'v''}$ is the transition wavelength, $A_{v'v''}$ is the state-to-state radiative decay rate, and the other symbols have their usual meanings. As pointed out by Morton and Noreau,²⁹ in the case of a $^1\Pi \leftarrow ^1\Sigma^+$ transition, the phenomenon of Λ -doubling has to be taken into account explicitly, and, since $\delta_{0\Lambda} = 1$ for Σ states and 0 otherwise, the degeneracy prefactor in Eq. (1) takes the value 2.

The radiative lifetime $\tau_{v'}^{\text{rad}}$ of the single vibrational level v' is given by

$$\frac{1}{\tau_{v'}^{\text{rad}}} = A_{v'} = \sum_{v''} A_{v'v''}^X + \sum_{e,v''} A_{v'v''}^e. \quad (2)$$

The summations in Eq. (2) take into account that the excited state may decay to many vibrational levels v'' of both the ground state X and other excited states e .

In the case of the $b^1\Pi_u(v=1)$ state, of principal interest here, dipole-allowed radiative decay can occur energetically, not only to the ground state $X^1\Sigma_g^+$, but also to the $a^1\Pi_g$, $a''^1\Sigma_g^+$, and $\Pi^1\Sigma_g^+$ states, the latter of which is only known theoretically.³⁰ The $b-a(1,0)$ transition has been observed experimentally.³¹ Inspection of Eq. (1) shows that, for a given oscillator strength, the contribution to the decay rate is inversely proportional to the square of the transition wavelength. Hence, there is likely to be a significantly smaller contribution from the $b^1\Pi_u-a''$, $\Pi^1\Sigma_g^+$ transitions, which occur in the far-IR and visible, respectively, than from the $b^1\Pi_u-a^1\Pi_g$ transition, which lies in the near-UV. Therefore, here we consider only the $b-X$ and $b-a$ decay channels and take the $b(v=1)$ radiative lifetime to be given by

$$\frac{1}{\tau_1^{\text{rad}}} = A_1 = \sum_{v''} A_{1v''}^X + \sum_{v''} A_{1v''}^a \quad (3)$$

Combining Eqs. (1) and (3), with appropriate degeneracy factors for the two electronic transitions, one may write

$$\frac{1}{\tau_1^{\text{rad}}} = A_1 = \frac{8\pi e^2}{4\epsilon_0 m_e c} \sum_{v''} \left[\frac{f_{1v''}^{bX}}{2(\lambda_{1v''}^{bX})^2} \right] + \frac{8\pi e^2}{4\epsilon_0 m_e c} \sum_{v''} \left[\frac{f_{1v''}^{ba}}{(\lambda_{1v''}^{ba})^2} \right] \quad (4)$$

In order to compute the oscillator-strength array for the $b-X$ transition, we employed the diabatic $^1\Pi_u$ potential-energy curves and couplings, and the $^1\Pi_u-X$ electronic transition moments of Spelsberg and Meyer³² in a rotationless, coupled-channel (CC) treatment of the Rydberg–valence and Rydberg–Rydberg interactions. As is well-known,⁹ the $^1\Pi_u-X$ oscillator strengths in N_2 display strong interference effects due to these interactions. As expected, our computed CC oscillator strengths $f_{v'0}^{bX}$ behave similarly to the band strengths computed by Spelsberg and Meyer,³² which correctly reproduce the *relative* trends in the experimental results of Geiger and Schröder.¹ However, it was necessary to scale the oscillator strengths by a factor of 0.75, equivalent to reducing the Spelsberg and Meyer transition moments by 13.4%, in order to optimize agreement with the absolute optical oscillator strengths of Stark *et al.*^{10,33} for the $b-X(v'=0-5,0)$ bands. These reduced diabatic electronic transition moments were used for all subsequent calculations of $f_{v'0}^{bX}$.

In Fig. 4, the computed $b-X(v'=0-5,0)$ oscillator strengths are compared with the absolute optical values of Stark *et al.*,³³ including a preliminary low- J value for the (5,0) band,¹⁰ and also with the electron-scattering intensities of Geiger and Schröder.¹ The latter are scaled to agree with the computed (4,0) oscillator strength of 0.0655. Agreement is excellent with each experimental data set and it is likely that the residual uncertainties in the computed oscillator strengths, and in the corresponding transition rates discussed below, are on the order of those applicable to the optical values to which they are scaled, i.e., $\sim 10\%$.

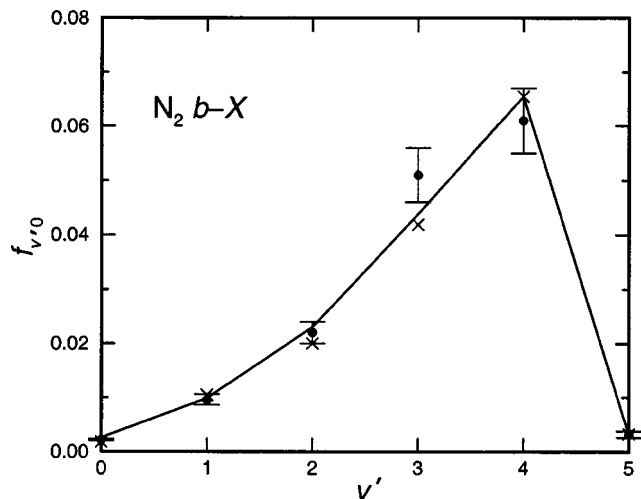


FIG. 4. Oscillator strengths for the $b-X(v'=0-5,0)$ bands. Solid line vertices: coupled-channel rotationless calculations, performed as described in the text. Solid circles: absolute optical values of Stark *et al.* (Refs. 10, 33). Crosses: electron-scattering values of Geiger and Schröder (Ref. 1), scaled to agree with the computed value for the (4,0) band.

Having thus “calibrated” our CC computational model, we then computed the oscillator strengths connecting $b(v=1)$ to the lowest 22 levels of the ground state, i.e., $f_{1v''}^{bX}$, which were then converted into the corresponding transition rates $A_{1v''}^X$ using the first term in Eq. (4). In Fig. 5, the computed relative fluorescence branching ratios $R_{1v''}^X = A_{1v''}^X / \sum_{v''} A_{1v''}^X$ are compared with the experimental branching ratios of James *et al.*³ and Zipf and Gorman.³⁴ In the range $v''=0-9$, excellent agreement is found with Zipf and Gorman,³⁴ and reasonable agreement with James *et al.*,³ but the (1,0) and (1,1) branching ratios of the latter work are not supported by the present calculations. The computed total transition rate from $b(v=1)$ to the first 22 levels of the ground state is $\sum_{v''} A_{1v''}^X = (2.60 \pm 0.26) \times 10^8 \text{ s}^{-1}$.

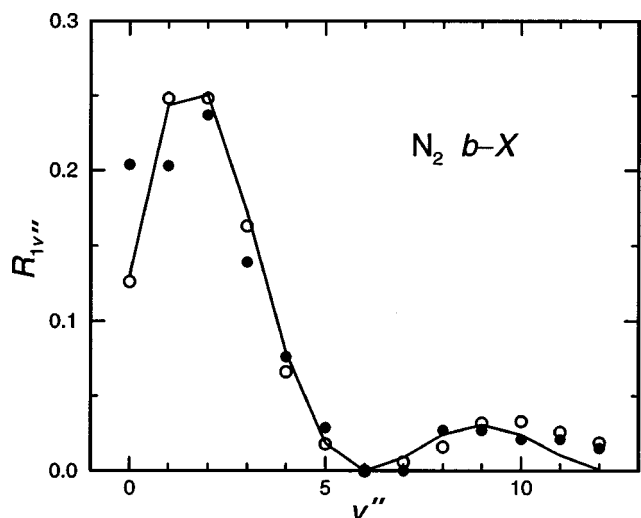


FIG. 5. Branching ratios for the $b-X(1,v'')$ fluorescence channels. Solid line vertices: coupled-channel rotationless calculations, performed as described in the text. Solid circles: experimental values of James *et al.* (Ref. 3). Open circles: experimental values of Zipf and Gorman (Ref. 34).

In principle, CC calculations should also be used to estimate the contribution of fluorescence to the $a^1\Pi_g$ state to the radiative lifetime of $b(v=1)$, but there is no information available on the magnitudes or phases of the corresponding diabatic electronic transition moments. Therefore, we performed an uncoupled, rotationless “adiabatic” calculation of the $b-a(1,v'')$ oscillator strengths, employing Rydberg–Klein–Rees potential-energy curves for the b and a states,³⁵ together with an R -dependent electronic transition moment assumed to be the same as that applying to the isoconfigurational $C^3\Pi_u-B^3\Pi_g$ transition.³⁶ The $b-a$ fluorescence is found to be dominated by the (1,0) transition, with significant contributions only for $v'' < 7$. The total transition rate, computed according to the second term in Eq. (4), is $\sum_v A_{1v''}^a = (0.17 \pm 0.09) \times 10^8\ \text{s}^{-1}$, only $\sim 7\%$ of the $b-X$ rate, with the large estimated relative uncertainty arising from the inevitable uncertainty in the assumed $b-a$ electronic transition moment.

Combining the computed rates for the two decay channels, we find a total transition rate $A_1 = (2.77 \pm 0.28) \times 10^8\ \text{s}^{-1}$, corresponding to a radiative lifetime $\tau_1^{\text{rad}} = 3.61 \pm 0.37\ \text{ns}$. The difference between this radiative lifetime and the observed lifetime of $2.61 \pm 0.10\ \text{ns}$ can be explained by residual predissociation of the $b(v=1)$ level. In the case of predissociation, the true lifetime is related to the radiative lifetime according to

$$\tau = \tau^{\text{rad}}(1 - \eta^{\text{pre}}), \quad (5)$$

where η^{pre} is the predissociation yield of the excited state. Using the present values for τ_1 and τ_1^{rad} in Eq. (5) gives an estimate for the predissociation yield of $\eta_1^{\text{pre}} = 0.28 \pm 0.10$. This value differs significantly from the value of 0.105 given by James *et al.*,³ but this disagreement is no cause for concern. James *et al.*³ derive their value from two quantities: an experimental emission cross section, with a stated uncertainty of 22%, and an excitation cross section which is scaled assuming a $b-X(4,0)$ band oscillator strength of 0.055, based on an old optical measurement.³⁷ If we rescale the excitation cross section of James *et al.*³ using our oscillator strength of 0.0655, based on a fit to more recent optical data,^{10,33} their emission cross section then implies a predissociation yield of 0.25 ± 0.30 , in good agreement with our result, but with a significantly greater uncertainty.

IV. CONCLUSIONS

A direct time-domain pump–probe lifetime measurement has been performed on the $b^1\Pi_u(v=1)$ level in $^{14}\text{N}_2$, yielding a lifetime of 2.61 ns. The measured lifetime is consistent with our coupled-channel calculation of the corresponding radiative lifetime, 3.61 ns, together with a predissociation yield of 28%.

In principle, a separate calculation of the predissociation lifetime is possible. However, the specific predissociation mechanisms for the dipole-accessible states of N_2 are yet to be identified, and, certainly, a comprehensive predissociation model is completely lacking. In any case, the reliable calculation of such a small predissociation linewidth ($\sim 0.0006\ \text{cm}^{-1}$ FWHM) for a single vibrational level among many

significantly broader levels would be very difficult. A predissociation model, including isotopic effects, and involving Rydberg–valence, Rydberg–Rydberg, spin–orbit, and rotational interactions, is currently being developed by some of the present authors. Our $b(v=1)$ predissociation-yield estimate may be useful in informing the development of that new predissociation model.

ACKNOWLEDGMENTS

J.P.S., W.U., and R.L. wish to thank the Lund Laser Center for their hospitality. This work was supported by the European Community, under the Access to Research Infrastructures initiative of the Improving Human Potential Program, Contract Nos. HPRI-CT-1999-00041 and HPRI-CT-1999-00064. Financial support from the Earth Observation (EO) program of the Space Research Organization Netherlands (SRON) and the Molecular Atmospheric Physics (MAP) program of the Netherlands Foundation for Research of Matter (FOM) is gratefully acknowledged. The authors thank P. Cacciani for help with the lifetime-fitting code, and I. Velchev for assistance during some of the measurements. G. Stark is also thanked for providing some of his unpublished results.

- ¹J. Geiger and B. Schröder, *J. Chem. Phys.* **50**, 7 (1969).
- ²E. C. Zipf and R. W. McLaughlin, *Planet. Space Sci.* **26**, 449 (1978).
- ³G. K. James, J. M. Ajello, B. Franklin, and D. E. Shemansky, *J. Phys. B* **23**, 2055 (1990).
- ⁴R. R. Meier, *Space Sci. Rev.* **58**, 1 (1991).
- ⁵H. Lefebvre-Brion, *Can. J. Phys.* **47**, 541 (1969).
- ⁶K. Dressler, *Can. J. Phys.* **47**, 547 (1969).
- ⁷P. K. Carroll and C. P. Collins, *Can. J. Phys.* **47**, 541 (1969).
- ⁸H. Lefebvre-Brion and R. W. Field, *Perturbations in the Spectra of Diatomic Molecules* (Academic, Orlando, 1986).
- ⁹D. Stahel, M. Leoni, and K. Dressler, *J. Chem. Phys.* **79**, 2541 (1983).
- ¹⁰G. Stark (private communication).
- ¹¹J. P. Sprengers, W. Ubachs, K. G. H. Baldwin, B. R. Lewis, and W.-Ü L. Tchchang-Brillet, *J. Chem. Phys.* **119**, 3160 (2003).
- ¹²M. Leoni and K. Dressler, *Z. Angew. Math. Phys.* **22**, 794 (1971).
- ¹³W. Ubachs, L. Tashiro, and R. N. Zare, *Chem. Phys.* **130**, 1 (1989).
- ¹⁴W. Ubachs, K. S. E. Eikema, and W. Hogervorst, *Appl. Phys. B: Photo-phys. Laser Chem.* **57**, 411 (1993).
- ¹⁵W. Ubachs, *Chem. Phys. Lett.* **268**, 201 (1997).
- ¹⁶W. Ubachs, I. Velchev, and A. de Lange, *J. Chem. Phys.* **112**, 5711 (2000).
- ¹⁷Y. Kawamoto, M. Fujitake, and N. Ohashi, *J. Mol. Spectrosc.* **185**, 330 (1997).
- ¹⁸H. Helm and P. C. Cosby, *J. Chem. Phys.* **90**, 4208 (1989).
- ¹⁹H. Helm, I. Hazell, and N. Bjerre, *Phys. Rev. A* **48**, 2762 (1993).
- ²⁰C. W. Walter, P. C. Cosby, and H. Helm, *J. Chem. Phys.* **99**, 3553 (1993).
- ²¹C. W. Walter, P. C. Cosby, and H. Helm, *Phys. Rev. A* **50**, 2930 (1994).
- ²²C. W. Walter, P. C. Cosby, and H. Helm, *J. Chem. Phys.* **112**, 4621 (2000).
- ²³B. Buijsse and W. J. van der Zande, *J. Chem. Phys.* **107**, 9447 (1997).
- ²⁴B. Buijsse and W. J. van der Zande, *Phys. Rev. Lett.* **79**, 4558 (1997).
- ²⁵H. Oertel, M. Kratzat, J. Imschweiler, and T. Noll, *Chem. Phys. Lett.* **82**, 552 (1981).
- ²⁶W. Ubachs, R. Lang, I. Velchev, W.-Ü L. Tchchang-Brillet, A. Johansson, Z. S. Li, V. Lohknygin, and C.-G. Wahlström, *Chem. Phys.* **270**, 216 (2001).
- ²⁷A. Johansson, M. K. Raarup, Z. S. Li, *et al.*, *Eur. Phys. J. D* **22**, 3 (2003).
- ²⁸P. Cacciani, F. Brandi, J. P. Sprengers, A. Johansson, A. L’Huillier, C.-G. Wahlström, and W. Ubachs, *Chem. Phys.* **282**, 63 (2002).
- ²⁹D. C. Morton and L. Noreau, *Astrophys. J., Suppl. Ser.* **95**, 301 (1994).
- ³⁰H. H. Michels, *Adv. Chem. Phys.* **45**, 225 (1981).
- ³¹K. J. Rajan, *Proc. R. Ir. Acad., Sect. A* **74**, 17 (1974).
- ³²D. Spelsberg and W. Meyer, *J. Chem. Phys.* **115**, 6438 (2001).

³³G. Stark, P. L. Smith, K. P. Huber, K. Yoshino, M. Stevens, and K. Ito, *J. Chem. Phys.* **97**, 4809 (1992).

³⁴E. C. Zipf and M. R. Gorman, *J. Chem. Phys.* **73**, 813 (1980).

³⁵A. Lofthus and P. H. Krupenie, *J. Phys. Chem. Ref. Data* **6**, 113 (1977).

³⁶F. R. Gilmore, R. R. Laher, and P. J. Espy, *J. Phys. Chem. Ref. Data* **21**, 1005 (1992).

³⁷G. M. Lawrence, D. L. Mickey, and K. Dressler, *J. Chem. Phys.* **48**, 1989 (1968).